

# Extension of the Karplus Relationship for NMR Spin–Spin Coupling Constants to Nonplanar Ring Systems: Pseudorotation of Cyclopentane

Anan Wu,<sup>†</sup> Dieter Cremer,<sup>\*,†</sup> Alexander A. Auer,<sup>‡</sup> and Jürgen Gauss<sup>‡</sup>

Department of Theoretical Chemistry, Göteborg University, Reutersgatan 2, S-41320 Göteborg, Sweden, and Institut für Physikalische Chemie, Universität Mainz, D-55099 Mainz, Germany

Received: August 15, 2001; In Final Form: November 5, 2001

A new Karplus equation for pseudorotating five-membered rings is derived by expanding calculated NMR spin–spin coupling constants (SSCCs)  $J$  as a function  $J(q,\phi)$  of the puckering amplitude  $q$  and the pseudorotational phase angle  $\phi$ . The approach was tested for cyclopentane but is equally applicable to ribose sugars and other biochemically interesting five-membered rings. It is based on the calculation of the conformational potential  $V(q,\phi)$ , which in the case of cyclopentane was determined at the MBPT(2)/cc-pVTZ level of theory. Cyclopentane is a free pseudorotor (barriers  $\Delta E$  and  $\Delta H \leq 0.01$  kcal/mol) with a puckering amplitude  $q = 0.43$  Å and a barrier to inversion  $\Delta H = 5.1$  kcal/mol, in perfect agreement with experimental data. The SSCCs of cyclopentane were calculated at MBPT(2)/cc-pVTZ geometries by use of coupled perturbed density functional theory (CP-DFT) with the B3LYP functional and a (9s,5p,1d/5s,1p)-[6s,4p,1d/3s,1p] basis set. In addition, coupled-cluster singles and doubles (CCSD) calculations were carried out to verify the CP-DFT results. All geometrical parameters and the 10 SSCCs of cyclopentane are determined as functions of the phase angle  $\phi$  and averaged to give  $\langle {}^nJ \rangle$  values that can be compared with experimental data. The following SSCCs (in hertz) were obtained at CP-DFT/B3LYP/[6s,4p,1d/3s,1p]:  $\langle {}^1J(\text{CC}) \rangle = 34.0$ ;  $\langle {}^1J(\text{CH}) \rangle = 127.6$ , exp 128.2;  $\langle {}^2J(\text{CCC}) \rangle = 2.3$ , exp (+)2.8;  $\langle {}^2J(\text{CCH}) \rangle = -2.6$ , exp (-)3.0;  $\langle {}^2J(\text{HCH}) \rangle = -12.4$ , exp (-)12.4;  $\langle {}^3J(\text{CCCH}) \rangle = 3.9$ ;  $\langle {}^3J(\text{HCCH}, \text{cis}) \rangle = 7.7$ , exp 7.7;  $\langle {}^3J(\text{HCCH}, \text{trans}) \rangle = 5.6$ , exp 6.3;  $\langle {}^4J(\text{HCCC}, \text{cis}) \rangle = 0.1$ ;  $\langle {}^4J(\text{HCCC}, \text{trans}) \rangle = -0.6$ . Magnitude and trends in calculated SSCCs are dominated by the Fermi contact term [with the exception of  ${}^1J(\text{CC})$ ]. A new way of determining puckering amplitude and pseudorotational angle by a combination of measured and calculated SSCCs is presented.

## 1. Introduction

Indirect nuclear magnetic resonance (NMR) spin–spin coupling constants (SSCCs) play an important role in the conformational analysis of biochemical compounds such as polypeptides and nucleic acids.<sup>1</sup> The dependence of measured SSCC values on the stereochemical relationship between the coupled nuclei is well documented both experimentally and theoretically.<sup>2–5</sup> In a series of investigations, Karplus rationalized the relative magnitude of vicinal SSCCs  ${}^3J(\text{HCCH})$  in dependence of the dihedral angle  $\tau(\text{HCCH})$  in terms of valence bond theory.<sup>2,3</sup> He derived a simple trigonometric relationship between  ${}^3J(\text{HCCH})$  and  $\tau(\text{HCCH})$ , which has been extensively used to determine dihedral angles and by this conformational features from measured SSCCs.<sup>1–5</sup> The so-called Karplus equation was established for different hydrocarbon fragments and extended by considering also substituent effects.<sup>6–8</sup>

Clearly, SSCCs depend also on other geometrical parameters in addition to the dihedral angle. For example, the absolute magnitude of the SSCC is reduced with increasing bond length (decreasing bond density), and similar changes are observed when the bond angles of a HCCH fragment change. However, the surface  ${}^nJ(R_i, \alpha_j, \tau_k)$  is much more complicated than the potential energy surface, which makes it in general difficult to relate changes in  ${}^nJ$  to a new set of internal coordinates  $\{R_i, \alpha_j, \tau_k\}$ . The Karplus relationship is based on the assumption that a change in the dihedral angle of a fragment HCCH of an acyclic

molecule implies only negligible changes in other geometrical parameters so that the dependence of SSCC on  $\tau$  can be exclusively considered.

Application of the Karplus relationship to pseudorotating rings should be in principle possible; however, it faces several problems. (a) In a pseudorotating ring, dihedral angles are limited to certain ranges where the upper boundary is given by the maximum degree of puckering. (b) While in an acyclic molecule a given proton can adopt both syn and anti positions relative to a given reference proton, this is not possible for the ring protons, which means that cis and trans relationships between ring protons have to be considered separately. (c) For a free or slightly hindered pseudorotor, experimentally only averaged SSCCs can be measured. Therefore, it is difficult to obtain sufficient information for setting up a Karplus relationship for pseudorotating ring molecules. (d) During pseudorotation of a ring all geometrical parameters change significantly, which means that a basic assumption of the Karplus relationship is no longer fulfilled.

In this work, we will extend the standard form of the Karplus equation  ${}^nJ(\tau)$  in the way that SSCCs of a nonplanar ring molecule are expressed as functions of the puckering coordinates of Cremer and Pople.<sup>9–16</sup> The final objective of this extension is the investigation of the conformations of biochemically interesting molecules such as ribose and 2'-deoxyribose sugars. We will establish the new type of Karplus equations for the SSCCs of cyclopentane. For this purpose, we will first determine the conformational potential  $V$  as  $V(q,\phi)$  for cyclopentane and

<sup>†</sup> Göteborg University.

<sup>‡</sup> Universität Mainz.

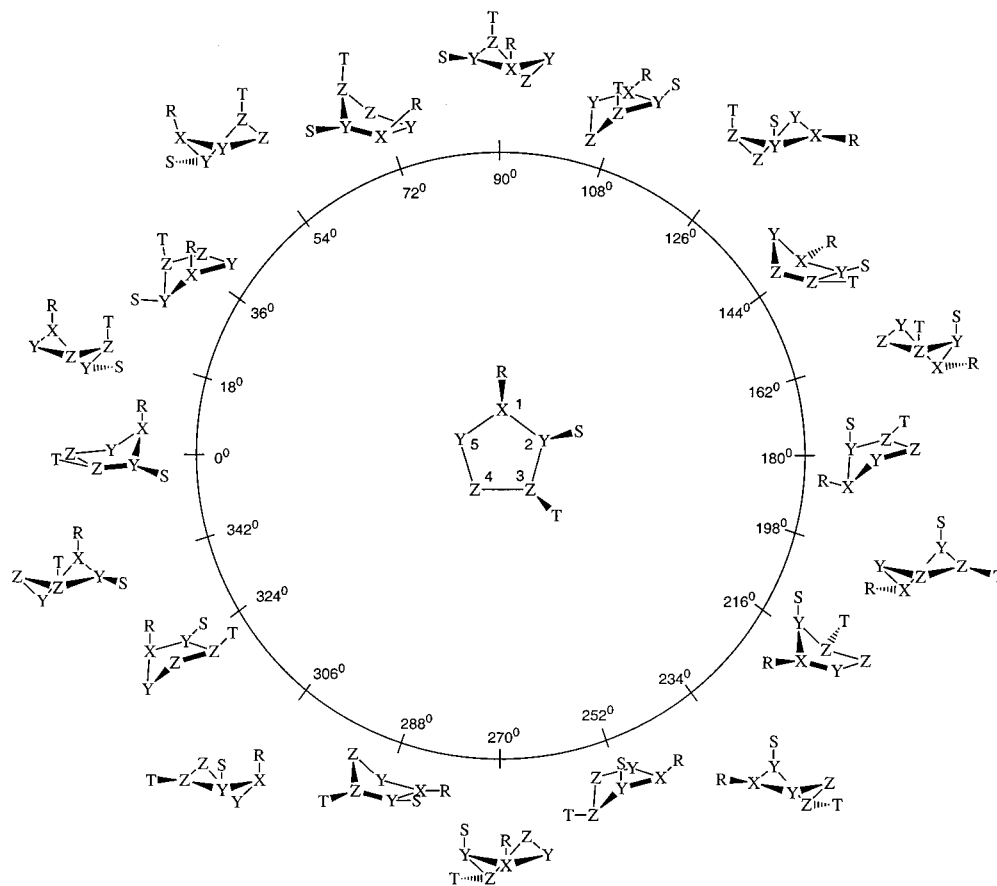


**Figure 1.** Pseudorotation itinerary ( $\phi = 0^\circ \rightarrow 360^\circ$ ) of a puckered five-membered ring such as cyclopentane. At the center ( $q = 0$ ), the planar ring is located. To distinguish different positions in the ring, symbols X, Y, Z (for ring atoms) and R, S, T (for substituents) are used.

characterize the molecule as a free pseudorotor. Then, we will calculate its SSCCs and determine those values that can be directly compared with measured SSCCs. The direct comparison of calculated and measured SSCCs will be the basis for the determination of the conformational features of puckered rings.

## 2. Computational Methods

According to the theory of ring puckering of  $N$ -membered rings developed by Cremer and Pople (CP),<sup>9</sup> the conformational space of a five-membered ring ( $N = 5$ ) is spanned by  $N - 3 = 2$  coordinates corresponding to a radial coordinate  $q$  determining the degree of ring puckering (puckering amplitude  $q = 0$  defines the planar form) and a pseudorotational coordinate  $\phi$  determining the mode of ring puckering [the pseudorotational phase angles  $\phi = (0 + k \times 360)/10$  for  $k = 0, 1, 2, \dots, 9$  and  $\phi = (18 + k \times 360)/10$  for  $k = 0, 1, 2, \dots, 9$  define the 10 envelope (E) and 10 twist (T) forms of cyclopentane for  $q > 0$  (see Figure 1)]. Any conformation of cyclopentane can be described as a linear combination of the two basis conformations E and T, while any conformational process of cyclopentane can be considered as a linear combination of ring pseudorotation and ring inversion through the planar ring form.<sup>9-16</sup>

The CP theory of ring puckering is based on the definition of a mean plane of the ring that is invariant during ring pseudorotation or any other conformational process. For a given conformation, the out-of-plane coordinates  $z_j$  of atoms  $j = 1, \dots, 5$  are defined by the puckering coordinates  $q$  and  $\phi$  according to<sup>9-13</sup>

$$z_j = \left(\frac{2}{5}\right)^{1/2} q \cos \left[ \frac{4\pi(j-1)}{5} + \phi \right] \quad (1)$$

for  $j = 1, \dots, 5$  and  $\phi[0;2\pi]$ , where the coordinates  $z_j$  are normalized according to

$$\sum_{j=1}^5 z_j^2 = q^2 \quad (2)$$

The Cartesian coordinates of any puckered  $N$ -membered ring are easy to calculate once  $N - 3$  puckering coordinates ( $N = 5$ ;  $q$  and  $\phi$ ),  $N - 3$  bond angles ( $N = 5$ ; two internal ring angles of the five-membered ring), and  $N$  (5) bond lengths are specified.<sup>12</sup> First, the  $z_j$  coordinates are calculated according to eq 1 (or similar formulas for  $N > 5$ ); then  $N$  bond lengths and  $N - 3$  bond angles projected onto the mean plane of the ring are determined. Finally, the coordinates  $x_j, y_j$  of the projected ring are calculated from  $2N - 3$  projected bond lengths and bond angles according to a procedure described by Cremer.<sup>12</sup>

The CP theory of ring puckering leads to considerable advantages for the conformational analysis of nonplanar rings.<sup>9-16</sup> In this work, we use this theory in the way that

(a) a given mode or degree of puckering of cyclopentane is defined with the help of the puckering coordinates;

(b) constrained geometry optimizations are carried out for fixed puckering coordinates (either  $\phi$  or both  $q$  and  $\phi$ ), which would not be possible if Cartesian or internal coordinates would be used;<sup>12</sup> and

(c) the properties of the five-membered ring (energy, geometrical parameters, SSCCs) are expressed as functions of the puckering coordinates.

In case b we use analytical gradients for ring puckering coordinates developed by Cremer.<sup>12</sup> These were also used to

calculate vibrational frequencies and to determine zero-point energies (ZPE) and enthalpies at 298 K,  $H(298)$ .

The conformational energy surface (CES) of cyclopentane was calculated by two different methods and three different basis sets. Preliminary geometry optimizations of the four conformations of cyclopentane investigated (planar form, E and T forms, and conformation with  $\phi = 9^\circ$ ) were carried out with second-order many-body perturbation theory [MBPT(2)] using the Møller–Plesset (MP) perturbation operator<sup>17</sup> and Dunning's cc-pVDZ basis set.<sup>18</sup> Conformational processes do not require high-level correlation methods because the bonding pattern remains unchanged during internal rotation, pseudorotation, etc. However, a reasonable account of ring strain and ring puckering requires that bond angle strain and in particular eclipsing/staggering of the CH bonds is correctly described, which are both influenced by the CC bond lengths. If the latter are underestimated, bond angle strain and eclipsing strain will be exaggerated and, by this, also the degree of ring puckering. Previous investigations revealed that MBPT(2) is sufficient to obtain a reasonable description of the CC bond lengths in cycloalkanes provided an extended basis set is used.<sup>11,19</sup> Hence, we repeated the MBPT(2) geometry optimizations with Dunning's cc-pVTZ basis set.<sup>18</sup>

Since the actual target of this project is the investigation of large ring systems such as ribose and 2'-deoxyribose sugars, for which MBPT(2)/cc-pVTZ calculations become too expensive in view of the large number of conformations that have to be calculated,<sup>20</sup> we tested also the performance of density functional theory (DFT)<sup>21</sup> in the present case. For this purpose, the hybrid functional B3LYP<sup>22–24</sup> in combination with Pople's 6-31G(d,p) basis set<sup>25</sup> was used.

The conformational potential  $V$  of any puckered five-membered ring can be expanded as a Fourier series in the phase angle  $\phi$ <sup>13</sup>

$$V(q, \phi) = \sum_{k=0}^{\infty} \{V_k^c(q) \cos(k\phi) + V_k^s(q) \sin(k\phi)\} \quad (3)$$

where  $V_k^c$  and  $V_k^s$  in turn can be expanded as Taylor series in the puckering amplitude  $q$ :

$$V_k(q) = \sum_{l=0}^{\infty} V_{kl} q^l \quad (4)$$

Previous computational investigations suggested free or slightly hindered pseudorotation for cyclopentane<sup>13,14,26,27</sup> in line with experimental results.<sup>28–31</sup> In view of these results and a 10-fold periodicity of the conformational potential of cyclopentane, the CES function can be expressed by

$$V(q, \phi) = V_{00} + V_{02}q^2 + V_{04}q^4 + V_{102}q^2 \cos(10\phi) + V_{104}q^4 \cos(10\phi) \quad (5)$$

where the constant  $V_{00}$  is set equal to the energy of the planar ring, which defines the zero point of the CES, i.e., puckering leads to a stabilization of cyclopentane. The determination of the unknown potential constants  $V_{02}$ ,  $V_{04}$ ,  $V_{102}$ , and  $V_{104}$  requires just two additional calculations, namely, those of the E and the T forms, because these forms occupy stationary points of the CES where the derivative of  $V(q, \phi)$  is equal to 0. In this work, a third nonplanar conformation halfway between the T and the E form [ $\phi = (9 + k \times 360)/10$  for  $k = 0, 1, 2, \dots$ ] was investigated to verify results based on the investigation of E and T form.

Since the maximum out-of-plane displacement rotates through the ring, atom C1 takes successively the five different positions in the ring. This is shown in Figure 1 where a limited number of cyclopentane conformations (separated by a  $\phi$  increment  $\Delta\phi = 18^\circ$ ) out of an infinite number of conformations along a fixed pseudorotation path is shown. Ring atoms are denoted as X, Y, and Z to identify specific positions in the ring and to reflect the symmetry of E ( $C_s$ ) and T ( $C_2$ ) form. Also, selected substituent positions are indicated by the symbols R, S, and T. Pseudorotation starts at  $\phi = 0^\circ$  where the E form with C1 = X, H(C1) = R, C2 = Y, etc., is located. At  $\phi = 90^\circ$  the T form with the same atom numbering is found, and at  $\phi = 180$  (270) $^\circ$  the inverted counterparts of E ( $\phi = 0^\circ$ ) and T ( $\phi = 90^\circ$ ) form. In the following we will define a given conformation by its  $\phi$  value and avoid the notation E and T, which is less specific (there are 10 different E and 10 different T forms, which in the case of cyclopentane become identical).

SSCCs were determined by coupled perturbed density functional theory (CP-DFT) as recently described and implemented by Cremer et al.,<sup>32</sup> who for the first time considered Fermi contact (FC), paramagnetic spin-orbit (PSO), diamagnetic spin-orbit (DSO), and spin-dipole (SP) terms consistently at the CP-DFT level of theory and showed that reliable SSCC values are obtained with the B3LYP functional.<sup>22–24</sup> In this work, the latter was employed in connection with Kutzelnigg's (9s,5p,1d/5s,1p)[6s,4p,1d/3s,1p] basis (basis II in ref 33).

For the purpose of testing the accuracy of CP-DFT SSCC values, we carried out also coupled-cluster calculations with all single and double excitations (CCSD) included.<sup>34,35</sup> Two basis sets were used in this connection, namely, a polarized double- $\zeta$  (dzp) basis with a (8s,4p,1d/4s,1p) [4s,2p,1d/2s,1p] contraction and a (11s,7p,2d/7s,2p) [6s,4p,2d/4s,2p] basis with valence quadruple- $\zeta$  double polarization (qz2p) character.<sup>36</sup>

By use of CP-DFT/B3LYP and CCSD, all SSCCs of the type  $J(^{13}\text{C}, ^{13}\text{C})$ ,  $J(^{13}\text{C}, ^1\text{H})$ , and  $J(^1\text{H}, ^1\text{H})$  were calculated, where for cost reasons only the FC contributions were determined in the case of the CCSD calculations. In the following, we will simplify the notation of SSCCs by using symbols such as  $^3J(\text{HCCH}, \text{cis})$  where C and H denote  $^{13}\text{C}$  and  $^1\text{H}$ , H–C–C–H the major coupling path of the 3-bond SSCC, and cis the positions of the H atoms on the same side of the ring. Important additional coupling paths will be identified by symbols  $^{n+m}J$  (coupling over  $n$  bonds and coupling over  $m$  bonds at the same time).

For pseudorotating ring molecules, only average SSCCs can be measured. For this purpose, one has to determine both the conformational potential and the SSCCs as a function of the pseudorotational phase angle  $\phi$  (or in general of all puckering coordinates). Assuming a Boltzmann distribution, the average SSCC is obtained according to

$${}^nJ(\text{average}) = \langle {}^nJ \rangle = \frac{\int_0^{2\pi} J(\phi) e^{-[V(\phi)-V(0)]/RT} d\phi}{\int_0^{2\pi} e^{-[V(\phi)-V(0)]/RT} d\phi} \quad (6)$$

In the case of a free pseudorotor,  $e^{-[V(\phi)-V(0)]} = 1$  and  ${}^nJ$  can be expressed as a periodic function in  $\phi$ :

$${}^nJ(\phi) = A + \sum_{i=1}^r B_i \cos(i\phi) + \sum_{j=1}^s C_j \sin(j\phi) \quad (7a)$$

Integration according to eq 6 leads to cancellation of the cosine and sine terms so that the average value is equal to constant  $A$  of eq 7a. In the case of a large amplitude vibration in the

**TABLE 1: Calculated Puckering Coordinates, Energies, and Enthalpies of Cyclopentane<sup>a</sup>**

method/basis	$\phi$	symbol	sym	q	energy $\Delta E$	H $\Delta H(298)$
B3LYP/6-31G(d,p)	planar	$D_{5h}$	0.000	-196.563 760	-196.418 163	
B3LYP/6-31G(d,p)	0	E	$C_s$	0.403	-4.58	-3.68
B3LYP/6-31G(d,p)	9		$C_1$	0.404	-4.57	-3.66
B3LYP/6-31G(d,p)	90	T	$C_2$	0.402	-4.60	-3.66
MP2/cc-pVDZ	planar	$D_{5h}$	0.000	-195.879 797	-195.733 318	
MP2/cc-pVDZ	0	E	$C_s$	0.432	-6.54	-5.56
MP2/cc-pVDZ	9		$C_1$	0.432	-6.54	-5.54
MP2/cc-pVDZ	90	T	$C_2$	0.432	-6.54	-5.54
MP2/cc-pVTZ	planar	$D_{5h}$	0.000	-196.087 385		
MP2/cc-pVTZ	0	E	$C_s$	0.429	-6.08	-5.10
MP2/cc-pVTZ	90	T	$C_2$	0.431	-6.08	-5.08
exp	0	E	$C_s$	0.438 <sup>b</sup>		-5.21 <sup>c</sup>

<sup>a</sup> Puckering amplitudes  $q$  are given in angstroms, absolute energies (enthalpies) in hartrees, and relative energies (enthalpies) in kilocalories per mole. Because of numerical inaccuracies the energy of the envelope (E) form cannot be exactly equal to the energy of the twist (T) form (deviations are in the range of  $10^{-6}$  Hartree) and therefore a first-order saddle point results for the E form as indicated by an imaginary frequency of  $13i$   $\text{cm}^{-1}$  for the pseudorotational mode. The corresponding value for the twist (T) form is  $9$   $\text{cm}^{-1}$  [MP2/cc-pVDZ;  $-16i$  and  $9$   $\text{cm}^{-1}$  at B3LYP/6-31G(d,p)]. Enthalpies at the MP2/cc-pVTZ level were calculated by using thermochemical corrections obtained at the MP2/cc-pVDZ level of theory. <sup>b</sup> Reference 31. <sup>c</sup> References 28 and 29.

direction of  $q$ , it is advantageous to replace eq 7a by

$${}^n J(q, \phi) = \sum_{k=0}^{\infty} \{ {}^n J_k^c(q) \cos(k\phi) + {}^n J_k^s(q) \sin(k\phi) \} \quad (7b)$$

with

$${}^n J_k(q) = \sum_{l=0}^{\infty} {}^n J_{kl} q^l \quad (7c)$$

where terms  ${}^n J_k(q)$  reflect the  $q$  dependence of constants  $A$ ,  $B_i$ , and  $C_j$  neglected in eq 7a. Equation 7b describes a new type of Karplus equation that can adopt in the case of cyclopentane or other free (slightly hindered) pseudorotors the form of eq 7a.

For the calculations, the program systems COLOGNE2000<sup>37</sup> and a local version of ACES II<sup>38</sup> containing CCSD modules for calculating spin-spin coupling constants were used.

### 3. The Flexible Pseudorotor Cyclopentane

Calculated energies and puckering coordinates obtained in this work are summarized in Table 1. The geometries of planar, E, and T forms are shown in Figure 2.

At the MBPT(2) level of theory, cyclopentane is predicted to be a free pseudorotor, i.e., all E and T forms have exactly the same energy and the same puckering amplitude (cc-pVDZ, 0.432 Å; cc-pVTZ,  $0.430 \pm 0.001$  Å; Table 1). This holds also for the conformation halfway between E and T form ( $\phi = 9^\circ$ ). The barrier to planarity  $\Delta E(\text{inv})$  is calculated to be 6.5 kcal/mol at MBPT(2)/cc-pVDZ and 6.1 kcal/mol at MBPT(2)/cc-pVTZ. This corresponds to an enthalpy difference at 298 K,  $\Delta H(298)$ , of 5.5 and 5.1 kcal/mol, respectively, in good agreement with experimental estimates of the barrier, all being close to 5.2 kcal/mol<sup>28,29</sup> (see Table 1 and footnotes given therein).

The puckering amplitude of cyclopentane was measured by electron diffraction (ED) techniques with a constrained model of the five-membered ring with equal CH and CC bond lengths and local  $C_{2v}$  symmetry of all  $\text{CH}_2$  groups.<sup>31</sup> The ED value of  $q_e = 0.438$  Å ( $\langle q \rangle = 0.427 \pm 0.015$  Å) is somewhat larger than the value of  $q_e = 0.431$  Å calculated for the T form at MBPT(2)/cc-pVTZ (Table 1). Luz and co-workers<sup>39</sup> calculated a  $\langle q \rangle$  value of 0.416 Å by combining ED data and NMR measurements of deuterated cyclopentane in liquid crystals. This corresponded to a  $q_e$  value of 0.463 Å, again with a rigid pseudorotor model.

Vibrational spectroscopy can also provide information about puckering and pseudorotation in cyclopentane; however, this information is rather indirect because it is based on a quantum chemical treatment of a rigid pseudorotor, i.e., all endo- and exocyclic bond lengths are constant during pseudorotation. The rigid pseudorotor assumption leads to an increase in ring strain and, accordingly, to larger puckering amplitudes. Durig and Willis<sup>30</sup> predicted a  $q$  value of 0.479 Å when they analyzed the infrared spectrum of cyclopentane with the help of a rigid pseudorotor model, while a similar approach based on the Raman spectra of cyclopentane led to 0.458 Å<sup>28</sup> and 0.47 Å.<sup>29</sup>

Previous quantum chemical investigations of cyclopentane were carried out at the molecular mechanics (MM) [ $\Delta E(\text{inv}) = 2.1$ – $4.7$  kcal/mol,  $q = 0.297$ – $0.444$  Å],<sup>26,27,40</sup> at the semi-empirical [AM1, PM3:  $\Delta E(\text{inv}) = 0.2$ – $0.6$  kcal/mol;  $q =$

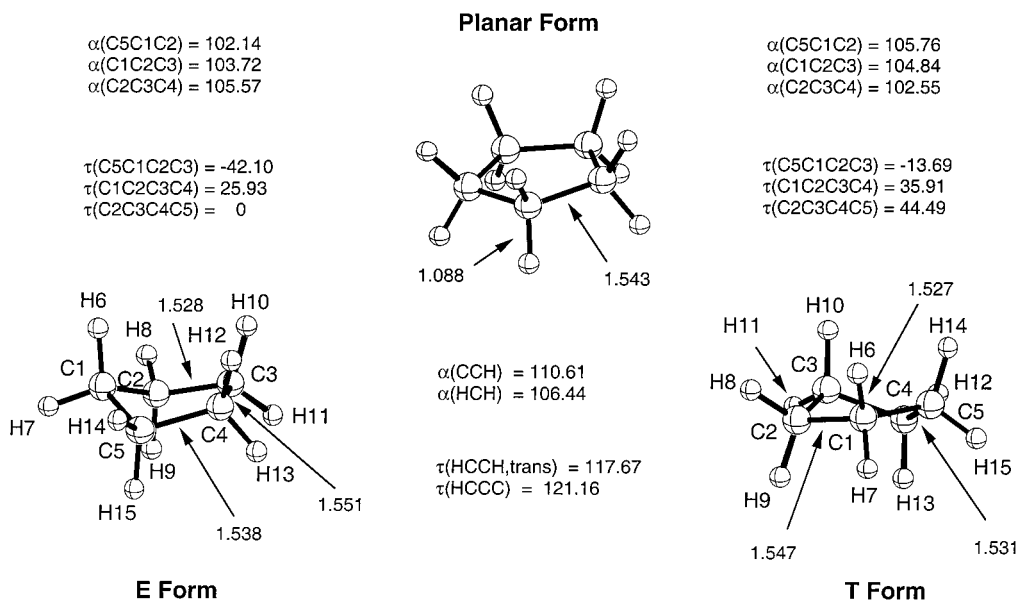


**Figure 2.** MBPT(2)/cc-pVTZ geometry of envelope (E), twist (T), and planar forms. Bond lengths are given in angstroms and angles in degrees.

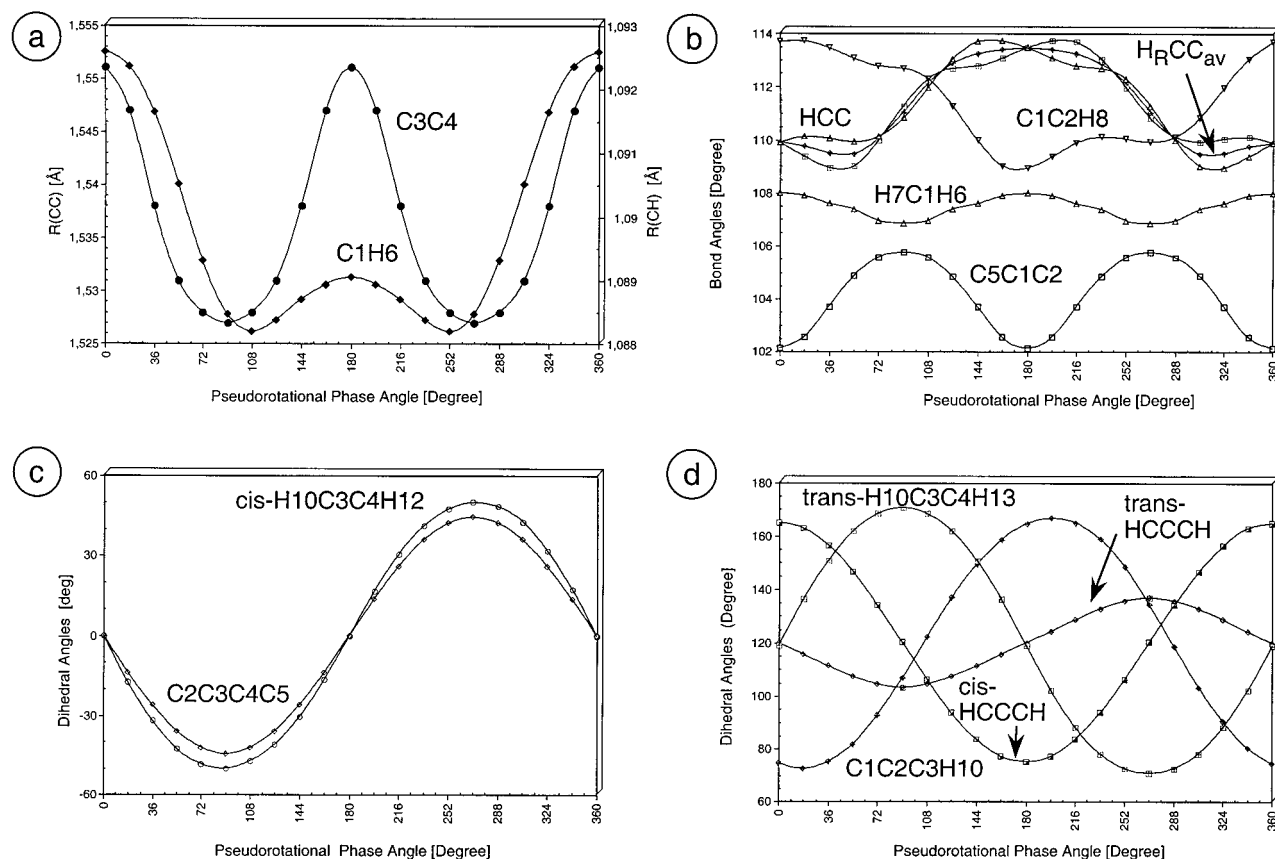


**Figure 3.** Dependence of the MBPT(2)/cc-pVTZ values of the internal coordinates of cyclopentane on the pseudorotational phase angle  $\phi$ . (a) Bond lengths  $R(\text{C3C4})$  and  $R(\text{C1H6})$ . (b) Bond angles  $\alpha(\text{C5C1C2})$ ,  $\alpha(\text{H7C1H6})$ , and  $\alpha(\text{C1C2H8})$ . In addition, the angles  $\alpha(\text{H6C1C2}) = \alpha_1$ ,  $\alpha(\text{H7C1C2}) = \alpha_2$ , and the average angle  $(\alpha_1 + \alpha_2)/2$  are given to facilitate the discussion of SSCCs. (c) Dihedral angles  $\tau(\text{C2C3C4C5})$  and  $\tau(\text{H10C3C4H12, cis})$ . (d) Dihedral angles  $\tau(\text{H10C3C4H13, trans})$ ,  $\tau(\text{C1C2C3H10})$ , and average HCCC dihedral angles of the units *cis*-H14C5C1C2H8 and *trans*-H15C5C1C2H8. For the Fourier expansion of internal coordinates of cyclopentane, see Table 2. The numbering of atoms is defined in Figure 2.

0.217–0.284 Å],<sup>26</sup> and at the Hartree–Fock (HF) level of theory [ $\Delta E(\text{inv}) = 4.1\text{--}5.0$  kcal/mol;  $q = 0.393\text{--}0.403$  Å].<sup>13,14,26</sup> Calculated pseudorotational barriers range from 0 to 1.1 kcal/mol.<sup>26</sup> Hence, all previous investigations were far from providing a reliable description of cyclopentane. Clearly, an electron-correlation corrected method is required to obtain a satisfactory description of the conformational features of cyclopentane.

DFT with the B3LYP functional provides a reasonable, though not accurate, account of pseudorotation in cyclopentane. The calculated puckering amplitude ( $q = 0.403 \pm 0.001$  Å, Table 1) is closer to the HF/6-31G(d,p) value of 0.403 Å,<sup>14,26</sup> while  $\Delta E(\text{inv}) = 4.6$  kcal/mol [ $\Delta H(\text{inv}, 298) = 3.7$  kcal/mol] is even smaller than the corresponding HF result (5.0 kcal/mol).

In Figure 3, calculated geometrical parameters of cyclopentane are given as a function of the pseudorotational phase angle  $\phi$  (see also Table 2). The largest changes are found for the dihedral angles:  $\tau(\text{CCCC})$ , 88.6°;  $\tau(\text{CCCH})$ , 94.5°;  $\tau(\text{HCCH, cis})$ , 102.3°; and  $\tau(\text{HCCH, trans})$ , 102.4°. These changes reflect the fact that the maximum  $\tau$ -values rotate through the ring similarly as the maximum out-of-plane deviation does during pseudorotation. Hence, if one focuses on one particular CC bond and its associated dihedral angles, the latter adopt all values between 0° and 44.3° (72.4° and 166.9°; 0° and 50°; 70.7° and 170.7°; Figure 3, Table 2) for  $\phi = 0^\circ \rightarrow 180^\circ$ .

The maximum amount of bond eclipsing takes place in the  $\text{H}_2\text{C3C4H}_2$  unit at  $\phi = 0^\circ$  and  $\phi = 180^\circ$ , thus leading to a relatively long bond, while the shortest C3C4 bond is found for  $\phi = 90^\circ$  and  $\phi = 270^\circ$  because the  $\text{CH}_2$  groups are largely staggered. The dihedral angles  $\tau(\text{HCCH, cis})$  can be increased

by 6° relative to  $\tau(\text{CCCC})$  because of a rocking movement of the  $\text{CH}_2$  groups (Figure 3c,d).

The changes in staggering/eclipsing interactions of the  $\text{CH}_2$  groups lead to a significant change in calculated CC bond lengths ( $\Delta = 0.024$  Å), which vary from 1.551 Å ( $\phi = 0^\circ$ ) to 1.527 Å ( $\phi = 180^\circ$ , Figure 3a). The CH bond lengths change only slightly (from 1.093 Å in axial positions to 1.086 Å in equatorial positions); however, these changes are nevertheless interesting in view of the changes in the calculated SSCCs. Two electronic effects are operative, namely, (a) a delocalization of the CH bonding electron pair from the  $\sigma(\text{CH})$  orbital into a vicinal  $\sigma^*(\text{CH})$  orbital (general anomeric effect) and (b) a hyperconjugative interaction between the pseudo- $\pi$  and pseudo- $\pi^*$  orbitals of the  $\text{H}_2\text{CCH}_2$  units (second-order hyperconjugation). The general anomeric effect operates when two vicinal CH bonds are in axial positions so that the  $\sigma(\text{CH})$  and  $\sigma^*(\text{CH})$  orbital can sufficiently overlap to make a delocalization of the CH bonding electrons possible. This leads to a weakening of the CH bonds but a strengthening of the CC bonds and is responsible for the fact that axial CH bonds are always longer than the equatorial CH bonds of cyclopentane, similar to the case of cyclohexane.<sup>11</sup>

The definition of ring substituent orientations given by Cremer<sup>10</sup> clarifies that, for  $\phi = 0^\circ \pm 72^\circ$ , C1H (X–R in Figure 1) is in an axial position while the equatorial position is adopted for  $\phi = 180^\circ \pm 36^\circ$ . In the latter case there is the largest degree of bond eclipsing, which via second-order hyperconjugation causes a lengthening of the CH bonds. The superposition of the two effects leads to the characteristic trend in the CH bond

**TABLE 2: Fourier Expansion for Geometrical and Magnetic Parameters of Cyclopentane<sup>a</sup>**

parameter	definition	A	$B_1 \cos \phi$	$B_2 \cos 2\phi$	$B_3 \cos 3\phi$	$B_4 \cos 4\phi$	$B_5 \cos 5\phi$	$C_1 \sin \phi$	$C_2 \sin 2\phi$	$C_3 \sin 3\phi$	std
$R(\text{CC})$	C3C4	1.5367	0.0002	0.0120							0.0019
$R(\text{CH})$	C1H6	1.0897	0.0018	0.0012							0.0001
$\alpha(\text{CCC})$	C5C1C2	104.12	-0.0075	-1.8544							0.14
$\alpha(\text{HCH})$	H6C1H7	107.45	-0.0018	0.5564							0.06
$\tau(\text{CCCC})$	C2C3C4C5	0						-44.2976			0.08
$\tau(\text{HCCH}, \text{cis})$	H10C3C4H12	0						51.1654	0.7766		0.93
$\tau(\text{HCCH}, \text{trans})$	H10C3C4H13	119.82		0.8238				51.1881			0.93
$^1J(\text{CC})$	C3C4	34.05	-0.0017	0.5545	0.0017	0.0456	0.0017				0.02
$^1J(\text{CH})$	C1H6	127.61	-2.6556	-0.1469	0.2109	-0.0456	0.0525				0.03
$^2J(\text{CCC})$	C5C1C2	2.33	0.0012	1.0382	0.0012	0.1669	0.0012				0.02
$^2J(\text{CCH})$	C1C2H8	-2.58	0.8884	-0.0969	0.1037			0.9865	0.2254	-0.2259	0.04
$^2J(\text{HCH})$	H6C1H7	-12.41	-0.0023	0.7493	-0.0023	-0.0263	0.0023				0.02
$^3J(\text{CCCH})$	C1C2C3H10	3.92	-2.5739	-0.6947	0.7301			-4.0056	1.7407	0.0318	0.13
$^3J(\text{HCCH}, \text{cis})$	H10C3C4H12	7.69	0.9253	3.1021	0.3828	0.2748					0.01
$^3J(\text{HCCH}, \text{trans})$	H10C3C4H13	5.61		0.9454		0.2866		6.6950		1.1957	0.06
$^4J(\text{HCCCH}, \text{cis})$	H14C5C1C2H8	0.1027	0.5598	0.4460	0.0414	-0.0257	0.0286				0.004
$^4J(\text{HCCCH}, \text{trans})$	H15C5C1C2H8	-0.5703		0.1454		0.0913		0.0853			0.02

<sup>a</sup> The Fourier expansion given in eq 7 was used. Coefficients  $B_i$  and  $C_j$  associated with  $\cos(i\phi)$  and  $\sin(j\phi)$ , respectively, are listed. Constant  $A$  corresponds to the average parameter  $\langle P \rangle$  or  $\langle {}^nJ \rangle$ . Bond lengths are given in angstroms, angles in degrees, and SSCCs  ${}^nJ$  in hertz. The numbering of atoms corresponds to that shown in Figures 1 and 2.

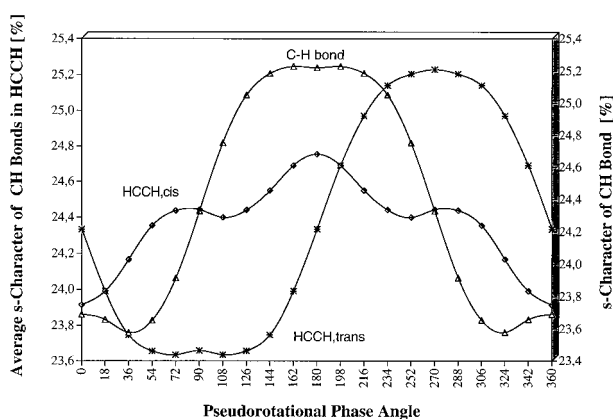


**Figure 4.** Dependence of the calculated s-character of the CH bond orbital (C1–H6 bond) of cyclopentane on the pseudorotational phase angle  $\phi$ . Also given are the average s-character of the two CH bond orbitals of the *cis*-HCCH and *trans*-HCCH fragments, H10C3C4H12 and H10C3C4H13 (see Figure 2).

lengths with minima at  $108^\circ$  and  $252^\circ$  and a small local maximum at  $\phi = 180^\circ$ .

Anomeric delocalization implies that the p-character of the CH bond orbitals increases. Hybrid orbitals calculated for cyclopentane with the NBO analysis<sup>41</sup> vary from  $sp^{3.53}$  ( $\phi = 0^\circ$ ) to  $sp^{3.28}$  ( $\phi = 180^\circ$ ), which (after normalization) corresponds to an increase in s-character from 23.7% to 25.2% when changing from an axial to an equatorial position for the CH bond (see Figure 4). There are no changes in the hybrid orbitals ( $sp^{2.64}$ ) forming the CC bonds of the ring during pseudorotation, which is of relevance when SSCCs are analyzed (see below).

The C5C1C2 bond angle changes by  $3.7^\circ$ , from  $102.1^\circ$  to  $105.8^\circ$  (Figure 3b), where a small angle is found for  $\phi = 0^\circ$  or  $180^\circ$  (E forms) and a larger one for  $\phi = 90^\circ$  or  $270^\circ$  (T forms). The HC1H angle is related to the C5C1C2 angle by the tetrahedral relationships, i.e., a small C5C1C2 angle implies a larger HC1H angle and vice versa, where, however, the variation in the exocyclic angle is just  $1.1^\circ$  (Figure 3b). This holds also for the corresponding HCC angles  $\alpha(\text{H}_6\text{C1C2}) = \alpha_1$ ,  $\alpha(\text{H}_7\text{C1C2}) = \alpha_2$ , and the average angle  $(\alpha_1 + \alpha_2)/2$  that are largest for the equatorially positioned CH bonds ( $\phi = 180^\circ \pm 36^\circ$ ) and smallest for the axial CH bonds ( $\phi = 0^\circ \pm 72^\circ$ , Figure 3b). In Figure 3d, the average of the HCCC dihedral angles in the fragments *cis/trans*-HCCCH are also given as a function of  $\phi$ , which are needed in the next section when SSCCs are analyzed.

**TABLE 3: Comparison of Calculated and Measured  $\langle {}^nJ \rangle$  Values of Cyclopentane<sup>a</sup>**

SSCC	$\langle {}^nJ \rangle$	exp value	comment	ref
$^1J(\text{CC})$	34.1	34.6	propane	8
$^1J(\text{CH})$	127.6	128.2	cyclopentane	48
$^2J(\text{CCC})$	2.3 (+)2.8		methylcyclopentane	8
$^2J(\text{CCH})$	-2.6 (-)3.0		cyclopentane	8
$^2J(\text{HCH})$	-12.4	-12.4 to -13.0	cyclopentane derivatives	48
$^3J(\text{CCCH})$	3.9	4.0	butane	8
$^3J(\text{HCCH}, \text{cis})$	7.7	7.7	cyclopentane	48
$^3J(\text{HCCH}, \text{trans})$	5.6	6.3	cyclopentane	48
$^4J(\text{HCCCH}, \text{cis})$	0.1			
$^4J(\text{HCCCH}, \text{trans})$	-0.6			

<sup>a</sup> All SSCCs  $\langle {}^nJ \rangle$  are given in hertz.

We conclude that the MBPT(2)/cc-pVTZ description of cyclopentane as a flexible pseudorotor is reliable and can be considered to provide a suitable basis to determine how the NMR SSCCs change with the pseudorotational phase angle. Each geometrical parameter of cyclopentane can be expressed as a function of the pseudorotational phase angle (Table 2) as shown for the SSCCs in eq 7a. In passing we note that a rigid pseudorotor model of cyclopentane that does not consider changes in the bond lengths leads to substantial errors; in particular it exaggerates the degree of ring puckering. This explains why spectroscopic investigations based on rigid pseudorotor models predict relatively large puckering amplitudes ( $q = 0.43\text{--}0.47 \text{ \AA}$ ).<sup>28–30,39</sup>

#### 4. Analysis of NMR Spin–Spin Coupling Constants

There are 10 different NMR SSCCs for cyclopentane: two  $^{13}\text{C}\text{--}^{13}\text{C}$ , three  $^{13}\text{C}\text{--}^1\text{H}$ , and five  $^1\text{H}\text{--}^1\text{H}$  SSCCs (see Table 2). The values of all SSCCs vary during pseudorotation in a typical way where the variation in the calculated values can be in the range of 1 up to 12 Hz (see Table 3). Although the sign is known for some of the SSCCs of cyclopentane, there are other SSCCs, for which the sign can only be guessed utilizing the Dirac vector model.<sup>1</sup> For cyclopentane, this model cannot guarantee reliability because (a) any measured SSCC is an average over individual SSCCs of conformations located along the pseudorotation path (an infinite number because of a barrier close to 0 kcal/mol; see eq 6) and (b) in ring systems more than one coupling path may contribute to the value of a given SSCC. This makes it very difficult to predict the sign of measured SSCCs for cyclopentane, and therefore, one goal of this work is to determine the signs of all SSCCs of cyclopentane.

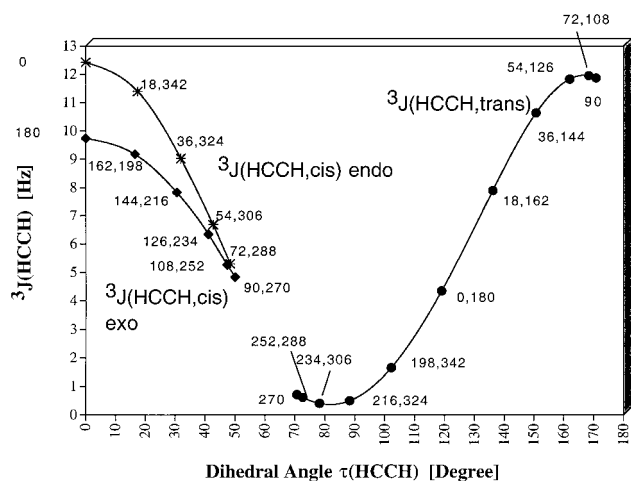


**Figure 5.** Dependence of the calculated SSCCs  $^3J(\text{HCCH})$  of cyclopentane on the dihedral angle  $\tau(\text{HCCH})$  (units H10C3C4H12 and H10C3C4H13, see Figure 2). For each SSCC, the corresponding  $\phi$  value is also given (compare with Figure 1).

### Is There a Typical Karplus Equation for Cyclopentane?

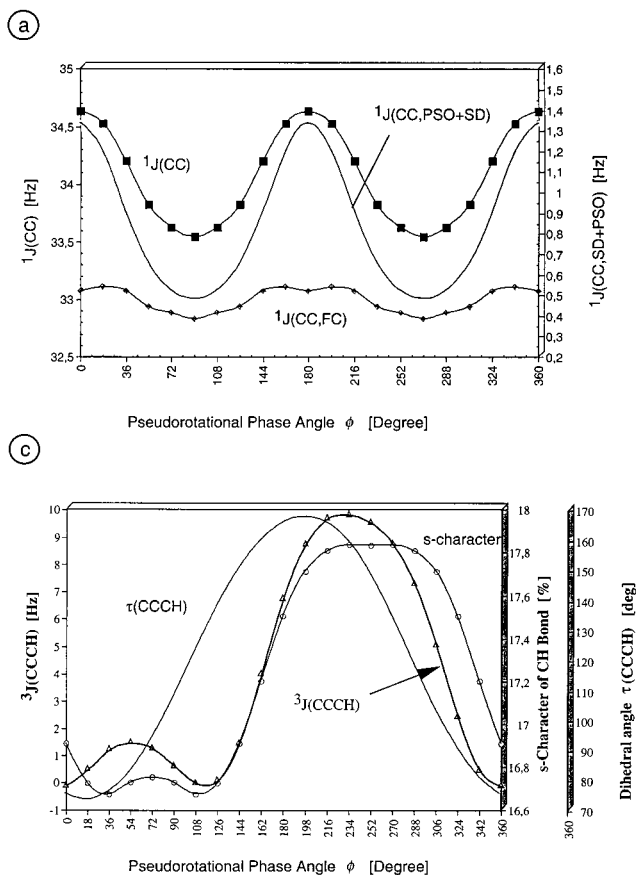
NMR investigations of cyclopentane and substituted cyclopentanes have focused in particular on the two  $^3J(\text{HCCH})$  constants, which should fit to the well-known Karplus relationships for vicinal H,H constants.<sup>1–8</sup> By representing  $^3J(\text{HCCH}, \text{cis})$  and  $^3J(\text{HCCH}, \text{trans})$  as a function of the associated dihedral angle  $\tau(\text{HCCH})$  (see Figure 5), two (rather than one) Karplus relationships are obtained because different conformations along the pseudorotation cycle possessing similar  $\tau(\text{HCCH})$  values lead to different  $^3J(\text{HCCH}, \text{cis})$  values. This difference is particularly large for the two E conformations at  $\phi = 0^\circ$  and  $\phi$

$= 180^\circ$ , for which  $\tau(\text{HCCH}) = 0$  in both cases. However, the *endo*-HCCH fragment has a SSCC of 12.4 Hz and the *exo*-HCCH fragment has a SSCC value of 9.7 Hz.

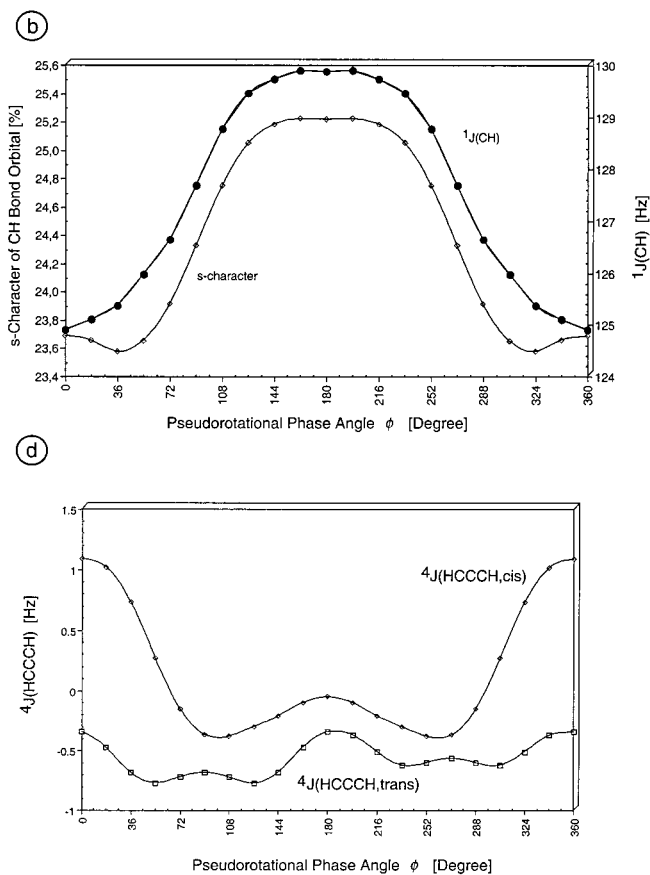
The difference of 2.7 Hz can be related to the well-known Barfield transmission effect,<sup>42</sup> which was extensively studied for the cyclopentane units of norbornane and for other molecules containing five-membered rings.<sup>42,43</sup> The origin of this effect is still a matter of dispute:<sup>44</sup> (a) Barfield and others<sup>42,43</sup> consider through-space interactions between the rear lobes of the CH bond orbitals in positions C3 and C4 with those at C1 responsible for a lowering of the *exo*  $^3J(\text{HCCH}, \text{cis})$  SSCC to 9.7 Hz. (b) Contreras and co-workers<sup>44</sup> emphasized that the difference between *endo* and *exo* couplings is almost fully described by the differences in the *bonds and antibonds containing the coupled protons*, where, however, the differences result from through-space interactions with the  $\text{CH}_2$  group opposite to the HCCH unit.

Attempts have been made to represent Barfield's transmission effect by an extra term in the normal Karplus equation.<sup>45</sup> Here, we pursue a different approach, which is based on the fact that any such effect also depends on the mode and degree of puckering (for  $q = 0$ , it vanishes) and, therefore, it will be automatically covered if  $^3J(\text{HCCH})$  is expressed as a function of the ring puckering coordinates of the five-membered ring rather than the dihedral angle  $\tau(\text{HCCH})$ . This leads to a new type of Karplus equation expressed as  $J(\phi)$  or  $J(q,\phi)$ .<sup>46</sup> The advantages of the latter formulation are the following:

- (1) The puckering coordinates identify uniquely each conformation of cyclopentane (in general, an  $N$ -membered puckered ring) in its two-dimensional  $[(N - 3)\text{-dimensional}]^9$  conformational space.
- (2) Expressing  $J$  as  $J(q,\phi)$  makes it easier to identify



**Figure 6.** Dependence of the calculated SSCCs  $J$  of cyclopentane on the pseudorotational phase angle  $\phi$ . For the definition of the molecular fragments associated with  $^nJ$ , see Table 2.



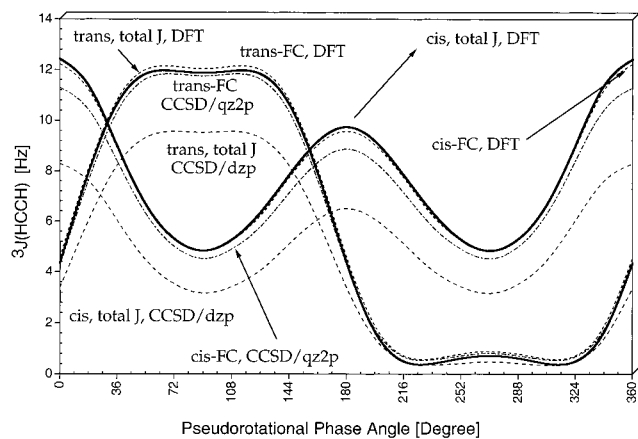


**Figure 7.** Dependence of the calculated SSCCs  ${}^3J(\text{HCCH})$  (units H10C3C4H12 and H10C3C4H13, see Table 2 and Figure 2) of cyclopentane on the pseudorotational phase angle  $\phi$ . CP-DFT results are given together with CCSD/dzp and CCSD/qz2p results, where in the latter case only the FC term was calculated. For reasons of comparison, this is also given for the CP-DFT results.

a given conformation by NMR measurements (preferably supported by suitable calculations such as the one performed in this work). (3) Each SSCC of the ring can be expressed in this way independent of whether it depends on a dihedral angle or not. (4) Since all geometrical parameters  $P$  of cyclopentane can also be expressed as functions  $P(q, \phi)$ , the analysis of measured (calculated)  $J$  values in terms of geometrical parameters  $P$  is considerably simplified. (5) The approach pursued in this work for cyclopentane can be easily extended to substituted cyclopentanes, other five-membered rings, or  $N$ -membered rings in general. (6) Measured and calculated  $J$  values can be combined to determine conformational features from suitable  $J(q, \phi)$  functions. In this way the use of NMR spectroscopy for determining molecular structure in the sense of the previously advertised NMR—*ab initio*—chemical shift method<sup>47</sup> can be significantly extended.

In the following we will discuss the 10 different SSCCs (Tables 2 and 3; for a definition of  $J$  constants, see Table 2) of cyclopentane where the emphasis will be on those  $J$  values that can be used to determine the puckering coordinates of cyclopentane and its derivatives.

**${}^1J(\text{CC})$  Constant.** This varies just by 1 Hz, between 34.6 and 33.5 Hz, during a pseudorotational cycle (Figure 7a), thus yielding an  $\langle {}^1J(\text{CC}) \rangle$  value of 34.0 Hz. This is comparable to the measured values for propane (34.6 Hz)<sup>8</sup> or cyclohexane (32.7 Hz);<sup>8</sup> the experimental value for cyclopentane is not known. The magnitude of the  ${}^1J(\text{CC})$  constant is largely determined by the FC term, which in turn depends on the  $s$ -character of the hybrid orbitals forming the CC bond.

**${}^1J(\text{CH})$  Constant.** The average SSCC value is 127.6 Hz, varying by 5 Hz between 124.9 Hz ( $\phi = 0^\circ$ ) and 129.9 Hz ( $\phi = 162^\circ$  and  $198^\circ$ ). The experimental value (128.2 Hz)<sup>48</sup> is just 0.6 Hz larger, indicating excellent agreement between measured and CP-DFT values. As can be seen from Figures 6b and 4, the variation in the  ${}^1J(\text{CH})$  value follows the changes in the  $s$ -character of the CH bond orbital.

**${}^2J(\text{CCC})$  Constant.** This SSCC changes only slightly, by 2 Hz from 1.4 Hz ( $\phi = 90^\circ, 270^\circ$ ) to 3.5 Hz ( $\phi = 0^\circ, 180^\circ$ ). To explain these variations, one has to consider that there are two coupling paths, thus yielding a  ${}^{2+3}J(\text{CCC}, \text{CCCC})$  SSCC, which depends on  $\tau(\text{CCCC})$  and therefore adopts large values for  $\phi = 0^\circ, 180^\circ$ . The calculated  $\langle {}^2J(\text{CCC}) \rangle$  value of 2.3 Hz agrees well with  $\langle {}^2J(\text{CCC}) \rangle = (+)2.8$  Hz measured for methylcyclo-

pentane,<sup>8</sup> where the sign of  ${}^2J(\text{CCC})$  was experimentally not determined. We note that  ${}^2J(\text{CCC})$  in cyclopentane, contrary to cyclohexane and cyclobutane,<sup>8</sup> is always positive.

**${}^2J(\text{CCH})$  Constant.** All calculated values are negative, varying between  $-1.1$  and  $-3.7$  Hz. The average value is  $-2.6$  Hz and compares well with an experimental value of 3 Hz, where the sign could not be determined but is assumed to be negative.<sup>8</sup> The variation of the SSCC follows the variation of the  $s$ -character of the CH bond in the way that larger  $s$ -character leads to more positive  ${}^2J(\text{CCH})$  values. Similar trends are found for the geminal H,H coupling constant.

**${}^2J(\text{HCH})$  Constant.** The SSCC varies only by 1.5 Hz, between  $-11.7$  Hz ( $\phi = 0^\circ, 180^\circ$ ) and  $-13.2$  Hz ( $\phi = 90^\circ, 270^\circ$ ). The variation is parallel to the changes in the average  $s$ -character of the two CH bond orbitals, which takes maximum values for  $\phi = 0^\circ$  and  $180^\circ$ . It is well-known that with an increase of the  $s$ -character more positive  ${}^2J(\text{HCH})$  values are obtained. The calculated value for  $\langle {}^2J(\text{HCH}) \rangle$  is  $-12.4$  Hz, which agrees well with a measured value of  $-12.4$  to  $-13.0$  Hz obtained for cyclopentane derivatives.<sup>48,49</sup>

**${}^3J(\text{CCCH})$  Constant.** In principle, this SSCC has to be considered as a  ${}^{3+4}J(\text{CCCH}, \text{CCCCH})$  constant because both coupling paths are possible. Its value is small for  $\phi = 0^\circ$  ( $-0.1$  Hz) and  $\phi = 108^\circ$  (0.02 Hz) and takes maximal values for  $\phi = 54^\circ$  (1.5 Hz) and  $\phi = 234^\circ$  (9.9 Hz, Figure 6c). The  $s$ -character of the CH bond orbital has a strong influence on the magnitude of the  ${}^3J(\text{CCCH})$  constant but would not explain by itself a variation of 10 Hz and other details of the function  ${}^3J(\phi)$  (Figure 6c). So the second important factor influencing the magnitude of this SSCC is due to the dihedral angle  $\tau(\text{CCCH})$ , which is close to  $170^\circ$  for  $\phi = 198^\circ$  but adopts values between  $75^\circ$  and  $105^\circ$  in the regions  $0^\circ \leq \phi \leq 90^\circ$  and  $306^\circ \leq \phi \leq 360^\circ$ . The calculated value of  $\langle {}^3J(\text{CCCH}) \rangle$  is 3.9 Hz. For cyclopentane this SSCC was not measured; however, for butanes, values between 4.0 and 5.4 Hz are known.<sup>8</sup>

**${}^3J(\text{HCCH})$  Constants.** The cis SSCC adopts large values for  $\tau(\text{HCCH}) = 0^\circ$  (12.4 and 9.7 Hz at  $\phi = 0^\circ$  and  $180^\circ$ ; Figure 7) and smaller values for  $\tau(\text{HCCH}) = 50^\circ$  (4.8 Hz for  $\phi = 90^\circ$  or  $270^\circ$ ). This is in line with a qualitative MO analysis, which predicts for cis and trans HCCH conformations a larger SSCC than for gauche HCCH conformations. As already discussed above, 1,3 through-space interactions lead to differences in the SSCCs for endo and exo HCCH fragments,<sup>42–45</sup> which are automatically covered when the SSCCs are expanded as functions of the puckering coordinates.

The variation in  ${}^3J(\text{HCCH}, \text{cis})$  during pseudorotation is reasonably described by a  $\cos \phi$  and a  $\cos 2\phi$  term (standard deviation 0.36 Hz) but requires for an accurate description also a  $\cos 3\phi$  and a  $\cos 4\phi$  term (standard deviation 0.01 Hz; see Table 2 and Figure 7). The value of  $\langle {}^3J(\text{HCCH}, \text{cis}) \rangle$  is calculated to be 7.7 Hz compared to measured values of 8.178 Hz ( $T = 290$  K), 8.130 Hz ( $T = 217$  K), and 7.987 Hz ( $T = 173$  K),<sup>48a</sup> from which a value of  $7.69 \pm 0.10$  Hz can be derived for  $T = 0$  K using a linear relationship. The latter value still includes vibrational effects; however, the difference between true equilibrium  $J$  constants and vibrationally averaged values should be small because of the averaging over an infinite number of cyclopentane conformers along the pseudorotation path. Hence, the agreement between theory and experiment is excellent in the case of  $\langle {}^3J(\text{HCCH}, \text{cis}) \rangle$ .

The changes in  ${}^3J(\text{HCCH}, \text{trans})$  along the pseudorotation path differ considerably from those of the corresponding cis SSCC. There are ranges of large ( $54^\circ \leq \phi \leq 126^\circ$ , 11.8 Hz) and small values of  ${}^3J(\text{HCCH}, \text{trans})$  ( $216^\circ \leq \phi \leq 324^\circ$ , 0.55



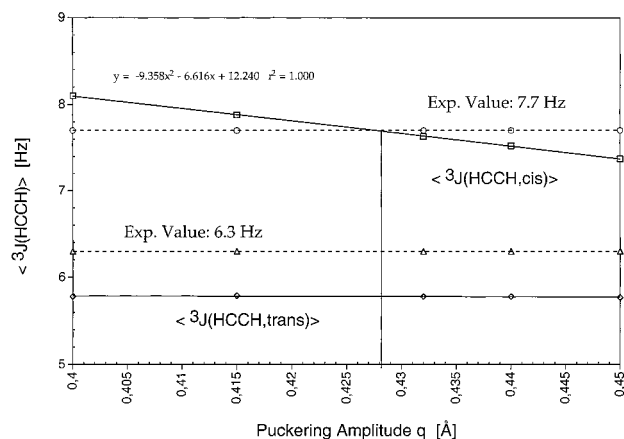


**Figure 8.** Dependence of the calculated SSCCs  $\langle {}^3J(\text{HCCH}) \rangle$  (units H10C3C4H12 and H10C3C4H13, see Table 2 and Figure 2) of cyclopentane on the puckering amplitude  $q$ . Experimental values are given for comparison. MBPT(2)/cc-pVDZ calculations were used.

$\pm 0.15$  Hz).  ${}^3J(\text{HCCH}, \text{trans})$  obviously depends on the dihedral angle  $\tau(\text{HCCH}, \text{trans})$  (Figures 3d and 5), according to which the largest (smallest) SSCC should be obtained for conformations with  $\phi = 90^\circ$  ( $270^\circ$ ). However, a second effect is superimposed on the first, leading to a broadening of the minimum and maximum of the  $\phi$  dependence of  ${}^3J(\text{HCCH}, \text{trans})$  and to a small local minimum (maximum) at  $\phi = 90^\circ$  ( $270^\circ$ ) (Figure 7). The second effect is caused by the s-character of the CH bond orbitals as can be seen from Figure 4, where the average s-character obtained for the two CH bond orbitals involved is plotted against the phase angle  $\phi$ .

A suitable Karplus equation for  ${}^3J(\text{HCCH}, \text{trans})$  is given in Table 2. The value of  $\langle {}^3J(\text{HCCH}, \text{trans}) \rangle$  based on this Karplus equation is 5.6 Hz, which has to be compared with the corresponding measured value of 6.3 Hz.<sup>48a</sup> Variation of the puckering amplitude  $q$  by 0.05 Å does not change the calculated  $\langle {}^3J(\text{HCCH}, \text{trans}) \rangle$  value (Figure 8). The temperature dependence of the measured value is smaller than that observed in the case of the corresponding cis value<sup>48a</sup> but would suggest a slightly larger rather than smaller SSCC at 0 K.

**${}^4J(\text{HCCCH})$  Constants.** There is a cis and a trans constant of this type depending on whether the H atoms are on the same (cis) or different (trans) sides of the ring. While the  ${}^4J(\text{HCCCH}, \text{cis})$  constant varies between 1.1 Hz ( $\phi = 0$ ) and  $-0.4$  Hz ( $\phi = 108^\circ$  and  $252^\circ$ , Figure 6d) the corresponding variation of the trans  ${}^4J(\text{HCCCH})$  constant is just 0.5 Hz and not very characteristic (Figure 6d). It is well-known that large  ${}^4J(\text{HCCCH})$  values are found for W-structures (anti,anti arrangement of bonds) and, therefore, the largest value of  ${}^4J(\text{HCCCH})$  is found for the cis constant at  $\phi = 0$  (see Figures 3d and 6d). If one plots the average of the two HCCC dihedral angles (denoted as *cis*-HCCCH in Figure 3d), then large values will be obtained for regions close to  $\phi = 0^\circ$  (indicating an anti-anti arrangement of bonds in the fragment H-C-C-C-H) and small values in the  $90^\circ \pm 90^\circ$  region of  $\phi$ , which indicates the range of relatively small cis SSCCs (Figure 6d). For the  ${}^4J(\text{HCCCH}, \text{trans})$  constant the corresponding average of HCCC dihedral angles (denoted as *trans*-HCCCH in Figure 3d) varies in the range  $120^\circ \pm 17^\circ$  in line with the fact that the trans value is always relatively small. The values for the  $\langle {}^4J(\text{HCCCH}) \rangle$  constants are 0.1 (cis) and  $-0.8$  Hz (trans). Experimental values are not known.

**Influence of FC, PSO, DSO, and SD Terms on Calculated SSCCs.** For all SSCCs of cyclopentane the magnitude is dominated by the FC term (see Figures 6 and 7) as is well-

known for hydrocarbons in general.<sup>1-3,8</sup> This holds also for most changes of the  $J$  values during pseudorotation. PSO, DSO, and SD terms also vary with  $\phi$ ; however, these variations are either relatively small or are such that the three terms cancel each other largely, thus leading to a small net effect on  $J$ . PSO and DSO term have mostly opposite signs and similar magnitudes so that their cumulative impact on the total SSCC is just 0.1–0.2 Hz.

The only exception from these general trends was found for  ${}^1J(\text{CC})$  (Figure 6a). In this case, the FC term again dominates the magnitude of the SSCC; however, the variation of  ${}^1J(\text{CC})$  during pseudorotation is caused by the PSO and SD terms, while FC and DSO contributions change only slightly. We connect the trends in the PSO and SD term with parallel trends in second-order hyperconjugation, which is large for the E forms at  $\phi = 0^\circ$  or  $180^\circ$  but small for the T forms at  $90^\circ$  and  $270^\circ$ . Second-order hyperconjugation involves the pseudo- $\pi$  and pseudo- $\pi^*$  orbitals of the  $\text{CH}_2$  groups and, contrary to the FC term, both the PSO and the SD term are sensitive to changes in the  $\pi$  density.

**Comparison with CCSD Results.** In view of the dominance of the FC contribution to the total NMR SSCCs of cyclopentane and in view of the relatively large cost of CCSD calculations, only the FC term of the most important SSCCs of cyclopentane was calculated. Test calculations for ethane indicate that the  $\text{d}_{\text{zp}}$  basis is too small for quantitative predictions. Thus, the CCSD/ $\text{qz}2\text{p}$  calculations are expected to provide the more reliable values, though quantitative calculations require even larger basis sets.

As shown in Figure 7, CP-DFT and CCSD calculations lead to the same dependence of the  ${}^3J(\text{HCCH})$  constants on the pseudorotational phase angle. At the CCSD/ $\text{d}_{\text{zp}}$  level both the FC(HCCH, *cis*) and FC(HCCH, *trans*) contributions are too small by about 3 Hz, which results in calculated average SSCCs (5.1 and 4.4 Hz) that are too low in comparison with experiment [exp FC(estimated) 7.8 and 6.5 Hz].<sup>50</sup> Similar observations were also made for other SSCCs of cyclopentane.

Use of the larger valence  $\text{qz}2\text{p}$  basis set leads to average FC values of 7.1 and 5.6 Hz, which are in better agreement with experiment. The CP-DFT results (7.8 and 5.8 Hz for the average FC contribution) are even closer to experiment than the CCSD/ $\text{qz}2\text{p}$  values. Due to the slow basis set convergence in the CCSD calculations of the FC term, it is difficult to predict a CCSD limit value for the FC contributions. In view of the reasonable agreement between the CCSD/ $\text{qz}2\text{p}$  and the CP-DFT results and considering the high computational cost of the CCSD calculations, the use of DFT is well justified and no further attempts were made to obtain SSCCs at the CCSD level of theory.

## 5. Chemical Relevance of Results

We have shown in this work that all SSCCs of cyclopentane are best described by a new type of Karplus equation given by eq 7b (or, in simplified form, by eq 7a) where  $J$  is expanded as function of the ring puckering coordinates, in particular the pseudorotational phase angle  $\phi$ .<sup>46</sup> In the case of free pseudorotation, the measured value of  $J$  corresponds to the constant  $A$  of the  $J(\phi)$  equation (Table 2; otherwise it has to be determined by integration as discussed in section 2). We will consider now how conformational features can be directly determined from  $\langle {}^nJ \rangle$  values.

**Determination of the Degree of Puckering.** For a free pseudorotor, the most interesting conformational parameter is the puckering amplitude  $q$ . Therefore, we investigated how the  $\langle J \rangle$  values depend on  $q$ . For this purpose, we repeated geometry

optimizations at the MBPT(2)/cc-pVDZ level of theory for fixed values of  $q$ , varying  $q$  in the range from 0.4 to 0.45 Å. The  ${}^3J(\text{HCCH})$  constants were calculated along the pseudorotation itinerary (with the same  $q$  value used for E and T form as pseudorotation turns out to be free for each  $q$  value chosen). Finally, the calculated values of  $\langle {}^3J(\text{HCCH}, \text{trans}) \rangle$  and  $\langle {}^3J(\text{HCCH}, \text{cis}) \rangle$  were given as a function of  $q$  (see Figure 8).

The values of  $\langle {}^3J(\text{HCCH}, \text{trans}) \rangle$  determined in this way do not show any significant dependence on  $q$  in the range of  $q$  values investigated. This is not surprising considering the dependence of  ${}^3J(\text{HCCH}, \text{trans})$  on  $\phi$  (see Figure 8): the region of a relatively large  ${}^3J(\text{HCCH}, \text{trans})$  values is mirror-imaged by a region of a relatively small  ${}^3J(\text{HCCH}, \text{trans})$  value. A decrease of  $q$  will reduce the large and increase the small  ${}^3J(\text{HCCH}, \text{trans})$  constants, thus leading to the same average value.

While  $\langle {}^3J(\text{HCCH}, \text{trans}) \rangle$  is not useful for determining  $q$ , the  $\langle {}^3J(\text{HCCH}, \text{cis}) \rangle$  values calculated in this work increase with decreasing  $q$ . The corresponding line crosses the experimental value of 7.7 Hz at  $q = 0.428$  Å, which is close to the MBPT(2)/cc-pVTZ value of  $q$  for the E form at  $\phi = 0^\circ$  ( $q = 0.429$  Å). Hence, one can use the measured *cis*-HCCH SSCCs to directly determine the degree of puckering of a cyclopentane from the information provided by the CP-DFT data of this work. We note that this approach is similar to the NMR—*ab initio*—IGLO method<sup>47</sup> used in connection with NMR chemical shift calculations to determine geometrical features of molecules in solution.<sup>51</sup>

**Determination of the Conformation from SSCCs.** In the case of alkyl- or aryl-substituted cyclopentanes, pseudorotation can be (partially or fully) hindered by barriers. Then, the question has to be answered: which conformations along the pseudorotation path occupy local minima of the CES? Since alkyl or aryl substituents will not change the Karplus equations determined in this work (provided there are no strong steric effects between the ring substituents),<sup>6–8</sup> one can use the equations of Table 2 to determine form and degree of puckering. In a first step, the pseudorotational potential  $V$  (see eq 3) of the cyclopentane derivative has to be determined where, depending on the size of the molecule, MBPT(2) (as in this work), DFT, or molecular mechanics calculations<sup>27</sup> can be applied, which all provide reasonable conformational potentials. Then,  $\langle J \rangle$  values are calculated from the functions  $J(q, \phi)$  (see eq 7 and Table 2). Applying the procedure described for cyclopentane leads to the determination of the puckering amplitude  $q$ .

Clearly, this approach can also be used to verify the conformational potential of a puckered ring and to determine in this way the most stable conformations. If pseudorotation is largely hindered by higher barriers, the stable conformations of the substituted cyclopentane can directly be identified by comparing measured SSCCs with the values given in this work. Helpful in this respect are particularly the three different vicinal SSCCs: A  ${}^3J(\text{CCCH})$  value larger than 2 Hz indicates a conformation in the range  $144^\circ \leq \phi \leq 324^\circ$ , while a value smaller than 2 Hz suggests a  $\phi$  between  $324^\circ$  and  $144^\circ$  (Figure 6c). The ratio  $R = {}^3J(\text{HCCH}, \text{cis})/{}^3J(\text{HCCH}, \text{trans})$  partitions these regions further (Figure 9): (a) for  $R$  close to 1,  $\phi = 36^\circ$  or  $162^\circ \pm 18^\circ$ ; (b) for  $R \leq 1$ ,  $\phi = 90^\circ \pm 40^\circ$ ; (c) for  $R$  very large,  $\phi = 225^\circ \pm 18^\circ$  or  $315^\circ \pm 18^\circ$ ; (d) for  $R = 6 \pm 3$ ,  $\phi = 198^\circ, 270^\circ$ , or  $0^\circ \pm 18^\circ$ . By use of additional relationships involving other SSCCs, these regions can be further partitioned. We note that such an approach was previously suggested on a purely qualitative basis.<sup>52</sup> Its quantification on the basis of this work is straightforward.

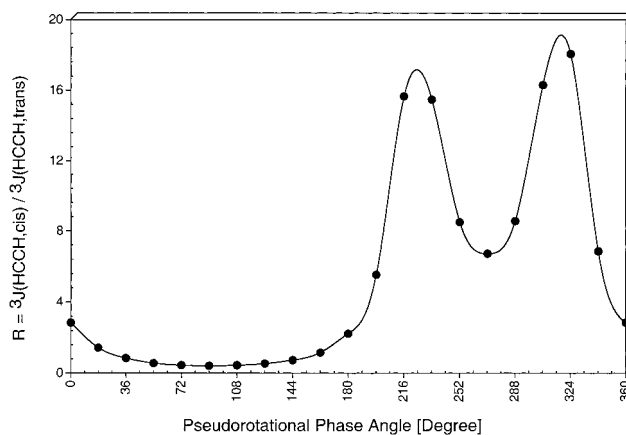


**Figure 9.** Dependence of the ratio  $R = {}^3J(\text{HCCH}, \text{cis})/{}^3J(\text{HCCH}, \text{trans})$  on the pseudorotational phase angle  $\phi$ .

In conclusion, the following results of this work have to be emphasized:

(1) Both puckering and pseudorotation of cyclopentane are reliably described at the MBPT(2)/cc-pVTZ level of theory. Cyclopentane is a free pseudorotor with a constant puckering amplitude of 0.43 Å and a barrier to ring inversion of 5.1 kcal/mol, thus confirming spectroscopic estimates of this barrier (5.2 kcal/mol).<sup>28,29</sup> Calculations show that spectroscopic estimates of the puckering amplitude based on a rigid pseudorotor model seriously exaggerate the puckering amplitude. An ED measurement of  $q$ ,<sup>31</sup> although also based on a simplified model of the pseudorotor molecule cyclopentane, leads to 0.438 Å ( $\langle q \rangle = 0.427 \pm 0.015$  Å), in reasonable agreement with the value calculated in this work. DFT/B3LYP does not reach the accuracy of the MBPT(2)/cc-pVTZ description of cyclopentane; however, calculated conformational parameters are reasonable so that the actual goals of this research, namely, the description of pseudorotation of ribose in DNA, can be pursued at the DFT level of theory.

(2) The CP-DFT/B3LYP calculations with the [6s,4p,1d/3s,1p] basis set provide SSCCs in excellent agreement with the available experimental values. Small deviations between measured and experimental values can be caused by vibrational effects not considered in this work. The CCSD/qz2p values of the FC contributions calculated for vicinal HCCH SSCCs support the CP-DFT results, although calculations reveal that CCSD SSCCs converge rather slowly with the basis set.

(3) The extension of the Karplus equation to puckered, pseudorotating ring molecules requires the use of the puckering coordinates. Once the new Karplus functions  $J(\phi)$  or  $J(q, \phi)$  are established, each conformation passed during pseudorotation of cyclopentane can be uniquely associated with a set of SSCCs. Since the geometrical parameters of the pseudorotating cyclopentane molecule can also be expressed as functions of the puckering coordinates, the analysis of SSCC in terms of geometrical parameters is straightforward.

(4) The FC term dominates both the magnitude and the variation of the SSCCs of cyclopentane during pseudorotation. PSO, DSO, and SD term also vary with  $\phi$ ; however, these variations are mostly small or cancel each other largely out. There is only one exception, namely, the SSCC  ${}^1J(\text{CC})$ , for which PSO and SD terms rather than the FC term dominate the variation in the total value of  $J$  during pseudorotation. The electronic effects causing the changes in the various SSCC contributions are discussed in this work.

(5) For the average values of the 10 SSCCs of pseudorotating cyclopentane, magnitude and sign are given in this work so that

NMR SSCCs previously not measured can now be determined. The variation of the SSCC of pseudorotating cyclopentane depends (a) on the dihedral angles and (b) on the change in the s-character of the CH bond orbitals. In several cases, additional coupling paths (through-bond and through-space) have to be considered. Noteworthy in particular is the difference of 2.7 Hz in the  ${}^3J(\text{HCCH}, \text{cis})$  values for endo and exo arrangements of HC3C4H at  $\phi = 0^\circ$ . This difference depends on the puckering amplitude  $q$  (decrease of the value for  $q \rightarrow 0$ ) and, if measurable, can also be used to determine the degree of puckering.

(6) The average values of the vicinal SSCCs  ${}^3J(\text{HCCH}, \text{cis})$  and  ${}^3J(\text{HCCH}, \text{trans})$  (7.7 and 5.6 Hz) agree well with the corresponding experimental values of 7.7 and 6.3 Hz.<sup>48</sup> In all other cases where experimental SSCCs are known for cyclopentane or methylcyclopentane, agreement between calculated and measured values is also excellent. However, this comparison is based on the assumption that vibrational effects for the averaged SSCCs are small.

(7) Determination of the puckering amplitude by a combination of the measured and calculated  ${}^3J(\text{HCCH}, \text{cis})$  average confirms a  $q$  value of 0.43 Å. Procedures are suggested to combine the functions  $J(q, \phi)$  and  $J(\phi)$  calculated in this work with measured NMR SSCCs to determine the conformers of substituted cyclopentanes which are no longer free pseudorotors.

The procedure developed in this work provides a basis to investigate the conformational behavior of biochemically interesting molecules such as ribose, 2'-deoxyribose, proline, etc. Work is in progress to accomplish this goal.

**Acknowledgment.** This work was supported at Göteborg by the Swedish Natural Science Research Council (NFR) and at Mainz by the Deutsche Forschungsgemeinschaft and the Fonds der Chemischen Industrie. Calculations were done on the supercomputers of the Nationellt Superdatorcentrum (NSC), Linköping, Sweden, and on local DEC workstations at the University of Mainz. D.C. thanks the NSC for a generous allotment of computer time.

## References and Notes

- (1) *Encyclopedia of Nuclear Magnetic Resonance*; Grant, D. M., Harris, R. K., Eds.; Wiley: Chichester, U.K., Vol. 1–8, 1996.
- (2) (a) Karplus, M.; Anderson, D. H. *J. Chem. Phys.* **1959**, *30*, 6. (b) Karplus, M. *J. Chem. Phys.* **1959**, *30*, 11.
- (3) Karplus, M. *J. Am. Chem. Soc.* **1963**, *85*, 2870.
- (4) (a) Kowalewski, J. *Prog. NMR Spectrosc.* **1977**, *11*, 1. (b) Kowalewski, J. *Annu. Rep. NMR Spectrosc.* **1982**, *12*, 81.
- (5) (a) Contreras, R. H.; Facelli, J. C. *Annu. Rep. NMR Spectrosc.* **1993**, *27*, 255. (b) Contreras, R. H.; Peralta, J. E. *Prog. NMR Spectrosc.* **2000**, *37*, 321.
- (6) (a) Altona, C. In *Encyclopedia of Nuclear Magnetic Resonance*; Grant, D. M., Harris, R. K., Eds.; Wiley: Chichester, U.K., 1996; p 4909. (b) Altona, C.; Sundaralingam, M. *J. Am. Chem. Soc.* **1973**, *95*, 2333. (c) Haasnoot, C. A. G. *J. Am. Chem. Soc.* **1993**, *115*, 1460.
- (7) For a review of ab initio SSCCs, see Helgaker, T.; Jaszunski, M.; Ruud, K. *Chem. Rev.* **1999**, *99*, 293 and references therein.
- (8) Kalinowski, H. O.; Berger, S.; Braun, S. *<sup>13</sup>C NMR-Spektroskopie*; Thieme: Stuttgart, Germany, 1984.
- (9) Cremer, D.; Pople, J. A. *J. Am. Chem. Soc.* **1975**, *97*, 1354.
- (10) Cremer, D. *Isr. J. Chem.* **1980**, *20*, 12.
- (11) Cremer, D.; Szabo, K. J. *Methods in Stereochemical Analysis, Conformational Behavior of Six-Membered Rings, Analysis, Dynamics, and Stereoelectronic Effects*; Juaristi, E., Ed.; VCH Publishers: Weinheim, Germany, 1995; p 59.
- (12) Cremer, D. *J. Phys. Chem.* **1990**, *94*, 5502.
- (13) Cremer, D.; Pople, J. A. *J. Am. Chem. Soc.* **1975**, *97*, 1358.
- (14) Cremer, D. *Isr. J. Chem.* **1983**, *23*, 72.
- (15) Cremer, D. *J. Chem. Phys.* **1979**, *70*, 1898, 1911, and 1928.
- (16) (a) Cremer, D. *Acta Crystallogr. B* **1984**, *40*, 498. (b) Essen, H.; Cremer, D. *Acta Crystallogr. B* **1984**, *40*, 418.
- (17) For a recent review see, Cremer, D. In *Encyclopedia of Computational Chemistry*; Schleyer, P. v R., Allinger, N. L., Clark, T., Gasteiger, J., Kollman, P. A., Schaefer, H. F., Schreiner, P. R., Eds.; Wiley: Chichester, U.K.; Vol 3, p 1706.
- (18) Dunning, T. H., Jr. *J. Chem. Phys.* **1989**, *99*, 1007.
- (19) Gauss, J.; Cremer, D.; Stanton, J. F. *J. Chem. Phys. A* **2000**, *104*, 1319.
- (20) Brameld, K. A.; Goddard, W. A. *J. Am. Chem. Soc.* **1999**, *121*, 985.
- (21) See, e.g., Parr, R. G.; Yang, W. *International Series of Monographs on Chemistry 16: Density-Functional Theory of Atoms and Molecules*; Oxford University Press: New York, 1989.
- (22) Becke, A. D. *J. Chem. Phys.* **1993**, *98*, 5648.
- (23) Becke, A. D. *Phys. Rev. A* **1988**, *38*, 3098.
- (24) Lee, C.; Yang, W.; Parr, R. P. *Phys. Rev. B* **1988**, *37*, 785.
- (25) Hariharan, P. C.; Pople, J. A. *Theor. Chim. Acta* **1973**, *28*, 213.
- (26) Han, S. J.; Kang, Y. K. *J. Mol. Struct. (THEOCHEM)* **1996**, *362*, 243.
- (27) Siri, D.; Gaudel, A.; Tordo, P. *J. Comput. Chem.* **2001**, in press.
- (28) Bauman, L. E.; Laane, J. *J. Phys. Chem.* **1988**, *92*, 1040.
- (29) Carreira, L. A.; Jiang, G. J.; Person, W. B.; Wills, J. N. *J. Phys. Chem.* **1972**, *56*, 1440.
- (30) Durig, J. R.; Willis, J. N. *J. Mol. Spectrosc.* **1969**, *32*, 320.
- (31) Adams, W. J.; Geise, H. J.; Bartell, L. S. *J. Am. Chem. Soc.* **1970**, *92*, 5013.
- (32) Sychrovsky, V.; Gräfenstein, J.; Cremer, D. *J. Chem. Phys.* **2000**, *113*, 3530.
- (33) Kutzelnigg, W.; Fleischer, U.; Schindler, M. In *NMR—Basic Principles and Progress*; Springer: Heidelberg, Germany, 1990; Vol. 23, p 165.
- (34) (a) Gauss, J.; Stanton, J. F. *Chem. Phys. Lett.* **1997**, *276*, 70. (b) Szalay, P. G.; Gauss, J.; Stanton, J. F. *Theor. Chem. Acc.* **1998**, *100*, 5.
- (35) Auer, A. A.; Gauss, J. *J. Chem. Phys.* **2001**, *115*, 1619.
- (36) Schäfer, A.; Horn, H.; Ahlrichs, R. *J. Chem. Phys.* **1992**, *97*, 257.
- (37) Kraka, E.; Gräfenstein, J.; Gauss, J.; He, Y.; Reichel, F.; Olsson, L.; Konkoli, Z.; He, Z.; Cremer, D. COLOGNE2000; Göteborg University: Göteborg, 2000.
- (38) Stanton, J. F.; Gauss, J.; Watts, J. D.; Lauderdale, W. J.; Bartlett, R. J. *Int. J. Quantum Chem. Symp.* **1992**, *26*, 879.
- (39) Joupko, R.; Luz, Z.; Zimmermann, H. *J. Am. Chem. Soc.* **1982**, *104*, 5307.
- (40) Rosas, R. L.; Cooper, C.; Laane, J. *J. Phys. Chem.* **1990**, *94*, 1830.
- (41) (a) Carpenter, J. E.; Weinhold, F. *J. Mol. Struct. (THEOCHEM)* **1988**, *169*, 41. (b) Reed, A. E.; Weinstock, R. B.; Weinhold, F. *J. Chem. Phys.* **1985**, *83*, 735. (c) Reed, A. E.; Curtiss, L. A.; Weinhold, F. *Chem. Rev.* **1988**, *88*, 899.
- (42) (a) Barfield, M. In *Encyclopedia of Nuclear Magnetic Resonance*; Grant, D. M., Harris, R. K., Eds.; Wiley: Chichester, U.K., 1996; p 2520. (b) Marshall, J.; Walter, S. R.; Barfield, M.; Marchand, A. P.; Marchand, N. W.; Segre, A. L. *Tetrahedron* **1976**, *32*, 537.
- (43) (a) Jaworski, A.; Ekiel, I.; Shugar, D. *J. Am. Chem. Soc.* **1978**, *100*, 4357. (b) Jaworski, A.; Ekiel, I. *Int. J. Quantum Chem.* **1979**, *16*, 615. (c) de Leeuw, F. A. A. M.; Altona, C.; Kessler, H.; Bermel, W.; Friedrich, A.; Krack, G.; Hull, W. E. *J. Am. Chem. Soc.* **1983**, *105*, 2237.
- (44) Cavasotto, C. N.; Giribert, C. G.; de Azua, M. C. R.; Contreras, R. H. *J. Comput. Chem.* **1991**, *12*, 141.
- (45) de Leeuw, F. A. A. M.; van Beuzekom, A. A.; Altona, C. *J. Comput. Chem.* **1983**, *4*, 438.
- (46) We note that steps in this direction have been made by Altona, Jaworski, and others (see, e.g., refs 43 and 45). However, these authors used approximate puckering coordinates valid only for the five-membered ring. Also, it was not recognized that any SSCC in any  $N$ -membered puckered ring can be expressed as a function of  $N - 3$  puckering coordinates.
- (47) (a) Cremer, D.; Olsson, L.; Reichel, F.; Kraka, E. *Isr. J. Chem.* **1993**, *33*, 369. (b) Ottosson, C. H.; Kraka, E.; Cremer, D. *Theoretical and Computational Chemistry, Volume 6, Pauling's Legacy—Modern Modeling of the Chemical Bonding*; Maksic, Z., Ed.; Elsevier: Amsterdam, 1999; p 231.
- (48) (a) Lipnick, R. L. *J. Mol. Struct.* **1974**, *21*, 411. (b) Lipnick, R. L. *J. Mol. Struct.* **1974**, *21*, 423.
- (49) Lipnick, R. L. *J. Am. Chem. Soc.* **1974**, *96*, 2941.
- (50) The FC contributions to measured  $\langle {}^3J(\text{HCCH}) \rangle$  values were estimated by scaling calculated  $\langle {}^3J(\text{FC}(\text{HCCH})) \rangle$  values by the ratio  $\langle {}^3J(\text{measured}) \rangle / \langle {}^3J(\text{calculated}) \rangle$ .
- (51) Cremer, D.; Reichel, F.; Kraka, E. *J. Am. Chem. Soc.* **1991**, *113*, 9459.
- (52) Constantino, M. G.; Silva, G. V. J. D. *Tetrahedron* **1998**, *54*, 11363.